Letter

Momentum space entanglement of interacting fermions

Michael O. Flynn,* Long-Hin Tang, Anushya Chandran, and Chris R. Laumann
Department of Physics, Boston University, 590 Commonwealth Avenue, Boston, Massachusetts 02215, USA

(Received 23 March 2022; revised 25 July 2022; accepted 30 January 2023; published 17 February 2023)

Momentum space entanglement entropy probes quantum correlations in interacting fermionic phases. It is very sensitive to interactions, obeying volume-law scaling in general, while vanishing in the Fermi gas. We show that the Rényi entropy in momentum space has a systematic expansion in terms of the phase space volume of the partition, which holds at all orders in perturbation theory. This permits, for example, the controlled computation of the entropy of thin shells near the Fermi wave vector in isotropic Fermi liquids and BCS superconductors. In the Fermi liquid, the thin-shell entropy is a universal function of the quasiparticle residue. In the superconductor, it reflects the formation of Cooper pairs. Momentum space Rényi entropies are accessible in cold atomic and molecular gas experiments through a time-of-flight generalization of previously implemented measurement protocols.

DOI: 10.1103/PhysRevB.107.L081109

Consider a many-body quantum system described by a wave function $|\psi\rangle$. For any partition of the system into regions A and $\bar{A}$, the nth Rényi entropy is

$$S_n(A) = \frac{1}{1-n}\ln \mathrm{Tr}\left[\rho_A^n\right], \tag{1}$$

where $\rho_A = \mathrm{Tr}_{\bar{A}}|\psi\rangle\langle\psi|$ is the reduced density matrix of subsystem A. Real space partitions have been extensively studied, as the scaling of $S_n(A)$ with the size of A characterizes ground state properties in equilibrium [1–4] as well as dynamical properties out of equilibrium [5–9]. The spectrum of eigenvalues of ρ_A can also probe the physical excitation spectrum [10] and the dynamical phase at nonzero temperature [11–13].

Real space Rényi entropy has been measured in systems of ultracold bosonic atoms [14,15] and trapped ions using several protocols [16,17]. Such measurements provide important experimental tests of quantum thermalization in isolated systems. Modified protocols have also been proposed for measuring real space entanglement in fermionic systems [18,19].

For translation-invariant fermionic systems, it is natural to consider partitions of $|\psi\rangle$ in momentum rather than real space (real space cuts are discussed in Refs. [4,20]). Momentum space entanglement is extremely sensitive to interactions: In the ground state of the noninteracting Fermi gas, $S_n(A) = 0$ for any momentum partition A. Generic interactions couple all momentum modes to one another, which implies that $S_n(A) \sim V|A|$, where V is the volume of the system and $|A|$ is the k-space volume of A (volume-law scaling) [21]. The entropy per mode, $s_n(A) \equiv S_n(A)/V|A|$, thus characterizes the effect of interactions in the system.

In this Letter, we compute $s_n(A)$ in the ground state of an isotropic Fermi system with short-range interactions [see Eq. (4)]. This model realizes a Fermi liquid when the interactions are repulsive and an s-wave superconductor when they are attractive. In both phases, the lowest energy modes lie in thin shells near the nominal Fermi wave vector k_F, which is a natural regime to search for universal phenomena (see Fig. 1 inset). Below, $A_{\delta k}$ denotes the set of modes with momenta in the range $[k_F - \delta k, k_F]$, and its spin-up (spin-down) polarized counterparts are $A^{\uparrow}_{\delta k}$ ($A^{\downarrow}_{\delta k}$).

We show that correlations between the different modes in $A_{\delta k}$ vanish as $\delta k \to 0$, such that the entropy $S_n(A_{\delta k})$ is simply the sum of the single mode entropies. In the main text, for simplicity, we argue that this holds within a certain *Gaussian approximation* for the interacting system. The Supplemental Material [22] generalizes this argument, relaxing the Gaussian approximation by using diagrammatic techniques to relate the entropy to the free energy of interacting fermions on pantslike manifolds (see Fig. 2).

In the Fermi liquid, as the single mode entropy arbitrarily close to the Fermi surface is characterized by the quasiparticle residue z_{k_F}, the Rényi entropies of thin-shell cuts have *universal* forms. For example, the second Rényi entropy is given by

$$s_2(A_{\delta k}) \underset{\delta k\to 0}{\longrightarrow} 2\ln\left[\frac{2}{1+z_{k_F}^2}\right] + O(\delta k/k_F). \tag{2}$$

In the s-wave superconductor, BCS theory predicts the presence of a superconducting gap Δ and Cooper pairing of fermions with opposite spin and momenta. Nontrivial momentum space partitions must trace out "half" of a Cooper pair; for partitions invariant under the transformation $\boldsymbol{k} \to -\boldsymbol{k}$, this requires that the partition is spin polarized. For $A^{\uparrow}_{\delta k}$, the second Rényi entropy is given by

$$s_2(A^{\uparrow}_{\delta k}) \simeq \begin{cases} \pi(1-2^{-1/2})\Delta/(v_F\delta k), & v_F\delta k \gg \Delta, \\ \ln 2, & v_F\delta k \ll \Delta, \end{cases} \tag{3}$$

where v_F is the Fermi velocity. The saturation to the value ln 2 reflects Cooper pairing throughout the thin shell. These results

*moflynn@bu.edu

 ©2023 American Physical Society

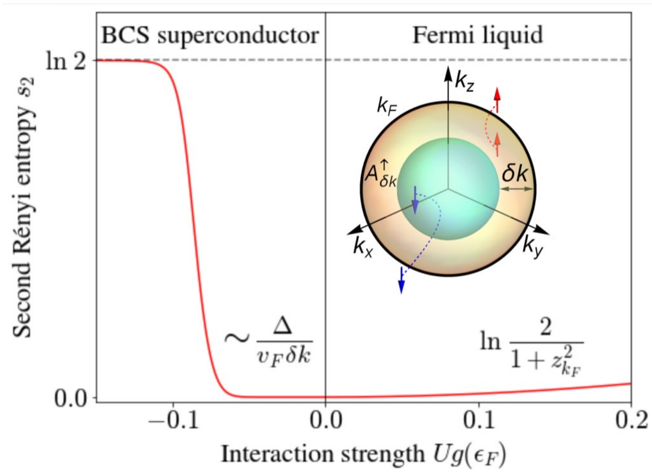

FIG. 1. The second Rényi entropy per mode $s_2(A^{\uparrow}_{\delta k})$ for a spin-polarized, thin-shell partition near the Fermi wave vector (inset). Here, $g(\epsilon_F)$ is the density of states at the Fermi energy, and the arrows in the inset indicate virtual processes that contribute to the entropy of the interacting ground state. The entropy is controlled by the quasiparticle residue z_{k_F} in the Fermi liquid, the gap Δ in the superconductor, and vanishes in the Fermi gas.

for the Fermi liquid and superconductor are summarized in Fig. 1.

Existing experimental protocols to measure real space entropy [16,17] can be simply generalized to momentum space, as the underlying procedures do not prefer a particular single-particle basis prior to final measurements. We discuss the generalized schemes further below. Several groups have measured single-atom-resolved correlations in momentum space in various ultracold bosonic and fermionic systems in the last few years [23–27], and have paved the way for the Rényi entropy measurements that we propose.

Momentum space entanglement has been previously studied in chiral and nonchiral fermionic systems. In the chiral quantum Hall setting, momentum space partitions are designed to probe the physics of a real space edge [10,28], so their physics is quite different. In a chiral nonlinear Luttinger liquid, quantum many-body scars may be diagnosed by their low momentum space entanglement entropies [29]. In the nonchiral setting, various features have been reported in model studies in disordered systems [30–33], related spin chains [34–36], Luttinger liquids [37,38], Hubbard models [39,40], and field theories [41–44].

Fermi liquids. Consider the following model of an isotropic Fermi liquid,

$$\begin{aligned} H &= H_0 + H_1, \\ H_0 &= \sum_{\boldsymbol{k},\sigma} \underbrace{(k^2/2m - \epsilon_F)}_{\xi_k} f^{\dagger}_{\boldsymbol{k}\sigma} f_{\boldsymbol{k}\sigma}, \\ H_1 &= \frac{U}{V} \sum_{\boldsymbol{k}_1+\boldsymbol{p}_1=\boldsymbol{k}_2+\boldsymbol{p}_2} f^{\dagger}_{\boldsymbol{k}_2\uparrow} f^{\dagger}_{\boldsymbol{p}_2\downarrow} f_{\boldsymbol{p}_1\downarrow} f_{\boldsymbol{k}_1\uparrow}, \end{aligned} \tag{4}$$

where $f^{\dagger}_{\boldsymbol{k}\sigma}$ ($f_{\boldsymbol{k}\sigma}$) are fermion creation (annihilation) operators with momentum $\boldsymbol{k}$ and spin σ, U is the interaction strength, and ϵ_F is the Fermi energy. Throughout this Letter, we take $|\psi\rangle$ to be the ground state.

Let us warm up by considering $A = \{\boldsymbol{k}\sigma\}$ a single spin-polarized mode. In this case, number conservation dictates that ρ_A is diagonal in the Fock basis with entries $\langle n_{\boldsymbol{k}\sigma}\rangle$ and $1 - \langle n_{\boldsymbol{k}\sigma}\rangle$. The single mode Rényi follows immediately,

$$S_n(\{\boldsymbol{k}\sigma\}) = \frac{1}{1-n} \ln[\langle n_{\boldsymbol{k}\sigma}\rangle^n + (1 - \langle n_{\boldsymbol{k}\sigma}\rangle)^n]. \tag{5}$$

If the mode lies near the Fermi surface, the occupation $\langle n_{\boldsymbol{k}\sigma}\rangle \approx (1 \pm z_{k_F})/2$ where we take $+$ $(-)$ for $\boldsymbol{k}$ inside (outside) the Fermi surface. Accordingly, the single mode entropy near the Fermi surface is an elementary function of the quasiparticle residue.

In general, going beyond a single mode is analytically challenging in an interacting state. As an approximate approach, we start by neglecting all multimode connected correlations. This "Gaussian approximation" to the Renyi entropy is computed by taking the true one-body density matrix

$$G_{\boldsymbol{k}'\sigma';\boldsymbol{k}\sigma} = \langle f^{\dagger}_{\boldsymbol{k}'\sigma'} f_{\boldsymbol{k}\sigma}\rangle \tag{6}$$

restricted to the modes in A and using the Peschel result for noninteracting fermions [45],

$$S^G_n(A) = \frac{1}{1-n} \operatorname{tr} \ln\left[G|_A^n + (\mathbf{1} - G|_A)^n\right]. \tag{7}$$

For the Fermi liquid, momentum and spin conservation dictate that $G|_A$ is already diagonal for $\boldsymbol{k}\sigma$-space cuts with eigenvalues given by the occupations $\langle n_{\boldsymbol{k}\sigma}\rangle$. With reference to Eq. (5), we find that the Gaussian approximation predicts that the Rényi entropy is simply the sum of the (exact) single mode entropies,

$$S^G_n(A) = \sum_{\boldsymbol{k}\sigma\in A} S_n(\{\boldsymbol{k}\sigma\}). \tag{8}$$

For general partitions A, this approximation is uncontrolled. For example, if A is the entire system, the true entropies vanish while Eq. (8) predicts an extensive positive value. On the other hand, S^G_n is clearly exact for A consisting of a single spin-polarized mode. More generally, short-range interactions in real space lead to long-range interactions in $\boldsymbol{k}\sigma$ space with an interaction strength that scales inversely with the volume V, as discussed in the Supplemental Material [22]. Perturbatively, the associated connected correlations vanish for finite sets of modes; we thus expect that the Gaussian approximation is accurate for sufficiently small cuts A in $\boldsymbol{k}\sigma$ space.

More precisely, in the Supplemental Material [22] we show that

$$S_n(A_{\delta k}) - \sum_{\boldsymbol{k}\sigma\in A_{\delta k}} S_n(\{\boldsymbol{k}\sigma\}) \sim O[(\delta k/k_F)^2] \tag{9}$$

holds to all orders in perturbation theory in the coupling U. Formally, we obtain this result by relating the various Rényi entropies in Eq. (9) to the free energy $F^{(n)}(W)$ of systems of interacting Grassmann fermions on pantslike manifolds in $\boldsymbol{k}\sigma$ space and imaginary time with varying waist regions W (see Fig. 2). Comparison of the diagrammatic expansion for $F^{(n)}$ on each of those manifolds allows us to show that the terms which contribute to Eq. (9) are indeed controlled by δk

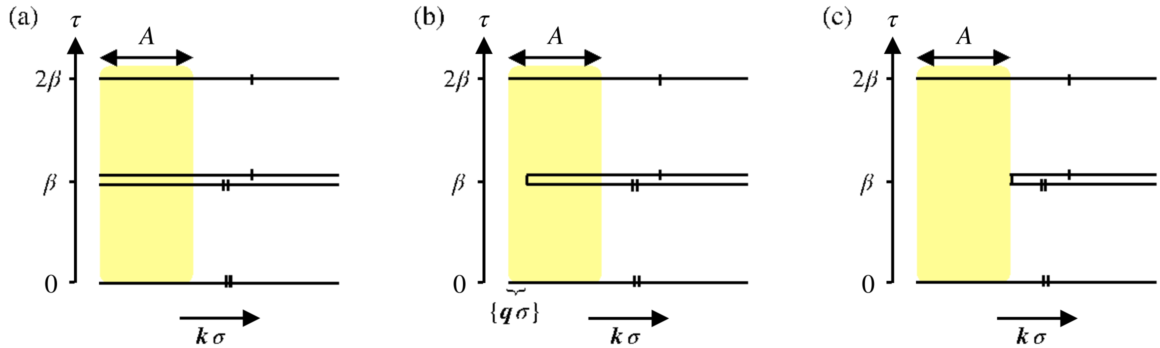

FIG. 2. The imaginary time manifold for pants in $\boldsymbol{k}\sigma$-τ space with various waists W, arising in the computation of the Rényi entropy: (a) the normalization free energy $F^{(n)}(\emptyset)$ ("tubes"), (b) the single mode Rényi free energy $F^{(n)}(\{\boldsymbol{q}\sigma\})$ ("low-rise jeans") and (c) the A Rényi free energy, $F^{(n)}(A)$ ("pants"), all shown for $n = 2$. The vertical axis shows imaginary time extending from 0 to $n\beta$, with boundaries cut and glued according to the markers. The horizontal axis is a schematic representation of $\boldsymbol{k}\sigma$ space.

at all orders. The reader might find it instructive to compare our approach with those of Refs. [46,47], which compute fermionic entropies without manifold embeddings.

Putting Eqs. (5), (8), and (9) together for a cut $A_{\delta k}$ near the Fermi surface recovers the universal result quoted in the introduction, Eq. (2).

Superconductors. As the Cooper pairs in an s-wave superconductor are composed of fermions with opposite spin and momentum, it is natural to focus on spin-polarized partitions $A^{\uparrow}$ of momentum space.

In this case, spin symmetry dictates that Eqs. (6)–(8) still provide the Gaussian approximation to the Renyi entropy. In particular, $G|_{A^{\uparrow}}$ is diagonal and the anomalous correlator $\langle f_{\boldsymbol{k}'\sigma'} f_{\boldsymbol{k}\sigma}\rangle$ vanishes when restricted to $A^{\uparrow}$. Note that the Gaussian approximation with nonvanishing anomalous correlators in A is different from that given in Eq. (7) (see, e.g., Ref. [45]).

Furthermore, as the discussion leading up to Eq. (9) suggests, the relationship between the single mode entropies and that of thin shells holds quite generally, although one needs to take into account symmetry breaking correctly. In the Supplemental Material [22], we show that Eq. (9) holds for spin-polarized partitions $A^{\uparrow}$ in the presence of s-wave superconducting order. In sum, the spin-polarized thin-shell Rényi entropies can be computed using Eqs. (7)–(9) as is.

Of course, in order to actually compute $S_n^G(A^{\uparrow})$, one needs to know the occupation numbers of the $\{\boldsymbol{k}\uparrow\}$ modes in the shell. BCS theory provides a self-consistent mean field approach to computing these occupations,

$$\langle f^{\dagger}_{\boldsymbol{k}\uparrow} f_{\boldsymbol{k}\uparrow}\rangle = \frac{1}{2}\left(1 - \frac{\xi_k}{\sqrt{\xi_k^2 + |\Delta|^2}}\right), \tag{10}$$

where $|\Delta|$ is the gap. Straightforward algebra produces

$$S_n(\boldsymbol{k}\uparrow) = \ln 2 + \frac{1}{1-n}\ln \sum_{r=0}^{\lfloor n/2\rfloor} \binom{n}{2r}\left(\frac{\xi_k^2}{\xi_k^2 + |\Delta|^2}\right)^r. \tag{11}$$

The scaling of $s_n(A^{\uparrow}_{\delta k})$ with $|\Delta|$ depends on its relative size with the energy scale of the thin shell. In the small gap limit $|\Delta| \ll v_F\delta k$, we can expand (11) in powers of $|\Delta/\xi_k|$ or $|\xi_k/\Delta|$ to obtain

$$S^n(\boldsymbol{k}\uparrow) \approx \begin{cases} \frac{n}{4(n-1)}\left|\frac{\xi_k}{\Delta}\right|^{-2}, & |\xi_k| > |\Delta|,\\ \ln 2 - n\left|\frac{\xi_k}{\Delta}\right|^{2}/2, & |\xi_k| < |\Delta|. \end{cases} \tag{12}$$

Summing up all contributions leads to the result in Eq. (3), which confirms the following simple intuition. When $|\Delta| \gg v_F\delta k$, all modes within the thin shell are strongly hybridized, resulting in the saturation of $s_n(A^{\uparrow}_{\delta k})$ to the maximal value $\ln 2$. On the other hand, when $|\Delta| \ll v_F\delta k$, $s_n(A^{\uparrow}_{\delta k})$ scales linearly in $|\Delta|/v_F\delta k$, since only modes within a region $|\Delta|$ around the Fermi surface are strongly hybridized.

Free Dirac transitions. Within BCS theory, the superconducting gap Δ exhibits an essential singularity at $Ug(\epsilon_F) = 0$. The thin-shell momentum space entropy shown in Fig. 1 inherits this singularity. It is natural to conjecture that this is connected to the presence of a spectral gap for $U < 0$, and that in analogy with real space entanglement, momentum space entropy can exhibit nonanalyticities in response to gap-inducing perturbations. We test this hypothesis by computing the second Rényi entropy of spin-polarized momentum balls around a Dirac point in D spatial dimensions. On tuning the mass m, we find a generic nonanalyticity

$$s_2(A^{\uparrow}) \sim |m|^D \ln |m| \tag{13}$$

in the free theory (see Supplemental Material [22]). We leave the extension to the interacting critical theory to future work.

Measurement protocol. A series of experiments with ultracold bosons have demonstrated that real space Rényi entropy can be measured by preparing copies of a quantum state and interfering them appropriately [14,15]. Here, we briefly review this protocol, which has been extended theoretically to fermionic systems as well [18,19], and generalize it to momentum space.

Begin with two identical copies of a quantum state in a pair of optical lattices; typically these are prepared by independent but identical time evolution in each copy. A beam splitter then interferes the two copies by freezing each of their dynamics and allowing for tunneling between them using an optical superlattice. This operation maps fermions in the first ($a^{\dagger}$) and second ($b^\dagger$) copies as

$$a_{i,\sigma}^\dagger \to \frac{a_{i,\sigma}^\dagger + b_{i,\sigma}^\dagger}{\sqrt{2}}, \quad b_{i,\sigma}^\dagger \to \frac{b_{i,\sigma}^\dagger - a_{i,\sigma}^\dagger}{\sqrt{2}}. \tag{14}$$

Microscopy techniques are then used to measure site and spin-resolved particle densities, from which the second Rényi entropy of an arbitrary real space partition is calculated [48].

Prior to measuring particle densities in real space, this protocol does not privilege any particular single-particle basis; it is the measurement basis which determines the partitions that can be accessed. Replacing real space microscopy with a time-of-flight (TOF) single-atom-resolved measurement [23–27] enables the computation of momentum space Rényi entropies in near-term experiments. In TOF, the atoms are released from the optical lattice and absorption imaging is used to reconstruct the initial momenta [49].

Discussion. We have shown that momentum space entanglement $S_n(A)$ in the ground state of interacting fermionic systems permits a systematic expansion in the phase space volume of A (shell width $\delta k \to 0$). This is analogous to the systematic expansion of the real space entanglement entropy in subsystem size $\ell \to \infty$.

In real space, the coefficient of the leading term is universal in gapless phases, where it captures the central charge in one-dimensional critical systems [1–3] and the geometry of the Fermi surface in higher D [4,20]. In momentum space, we find that the leading contribution to the entanglement entropy of thin shells near the Fermi surface depends only on the quasiparticle residue z_{k_F}. An interesting avenue for future work is to compute the $O(\delta k^2)$ contribution, where we expect the Landau parameters to play a role as they reflect the correlations between k modes.

The one-dimensional interacting Fermi system realizes a Luttinger liquid where $z_{k_F} = 0$. Despite the more dramatic reorganization of the ground state from the noninteracting Fermi sea, we nonetheless expect $s_2(A_{\delta k}) = 2\ln 2 + O(\delta k)$. This follows by applying our results to the parquet-diagram based perturbative treatment of the Luttinger liquid [50]; it would be interesting to check this in a direct multimode calculation, building on Ref. [36].

The detailed understanding of real space entanglement has fed into great improvements in matrix-product based numerical techniques [51–53]. As the phase space expansion gives systematic control of entanglement in momentum space, we expect similar positive feedback on the development of momentum space based algorithms [40,54–56]. Separately, momentum space based quantum Monte Carlo techniques on manifolds of the type in Fig. 2 should give direct access to thin-shell entropies [57–59].

Our diagrammatic proof shows that the leading term in δk is given by the sum of the exact single mode entropies for short-range interactions and choices of spin polarization in the thin shell A. We expect these arguments can be extended to Coulomb interactions and more complicated symmetry breaking patterns. This paves the way to systematically explore momentum space entanglement in more complicated phases such as unconventional superconductors, antiferromagnets, and electron nematics.

Acknowledgments. The authors are grateful to M. Bellitti, C. Chamon, G. Goldstein, D. Long, and A. Nahum for stimulating discussions. This work was supported by the Air Force Office of Scientific Research through Grant No. FA9550-16-1-0334 (M.O.F.) and by the National Science Foundation through Awards No. DMR-1752759 (L.-H.T. and A.C.) and No. PHY-1752727 (C.R.L.).

[1] J. Eisert, M. Cramer, and M. B. Plenio, Colloquium: Area laws for the entanglement entropy, Rev. Mod. Phys. **82**, 277 (2010).

[2] G. Vidal, J. I. Latorre, E. Rico, and A. Kitaev, Entanglement in Quantum Critical Phenomena, Phys. Rev. Lett. **90**, 227902 (2003).

[3] P. Calabrese and J. Cardy, Entanglement entropy and quantum field theory, J. Stat. Mech.: Theory Exp. (2004) P06002.

[4] D. Gioev and I. Klich, Entanglement Entropy of Fermions in Any Dimension and the Widom Conjecture, Phys. Rev. Lett. **96**, 100503 (2006).

[5] P. Calabrese, J. Cardy, and B. Doyon, Entanglement entropy in extended quantum systems, J. Phys. A: Math. Theor. **42**, 500301 (2009).

[6] T. Grover, Y. Zhang, and A. Vishwanath, Entanglement entropy as a portal to the physics of quantum spin liquids, New J. Phys. **15**, 025002 (2013).

[7] N. Laflorencie, Quantum entanglement in condensed matter systems, Phys. Rep. **646**, 1 (2016).

[8] L. D'Alessio, Y. Kafri, A. Polkovnikov, and M. Rigol, From quantum chaos and eigenstate thermalization to statistical mechanics and thermodynamics, Adv. Phys. **65**, 239 (2016).

[9] D. A. Abanin, E. Altman, I. Bloch, and M. Serbyn, Colloquium: Many-body localization, thermalization, and entanglement, Rev. Mod. Phys. **91**, 021001 (2019).

[10] H. Li and F. D. M. Haldane, Entanglement Spectrum as a Generalization of Entanglement Entropy: Identification of Topological Order in Non-Abelian Fractional Quantum Hall Effect States, Phys. Rev. Lett. **101**, 010504 (2008).

[11] V. A. Marčenko and L. A. Pastur, Distribution of eigenvalues for some sets of random matrices, Math. USSR-Sb. **1**, 457 (1967).

[12] S. C. Morampudi, A. Chandran, and C. R. Laumann, Universal Entanglement of Typical States in Constrained Systems, Phys. Rev. Lett. **124**, 050602 (2020).

[13] S. D. Geraedts, N. Regnault, and R. M. Nandkishore, Characterizing the many-body localization transition using the entanglement spectrum, New J. Phys. **19**, 113021 (2017).

[14] R. Islam, R. Ma, P. M. Preiss, M. Eric Tai, A. Lukin, M. Rispoli, and M. Greiner, Measuring entanglement entropy in a quantum many-body system, Nature (London) **528**, 77 (2015).

[15] A. M. Kaufman, M. E. Tai, A. Lukin, M. Rispoli, R. Schittko, P. M. Preiss, and M. Greiner, Quantum thermalization through entanglement in an isolated many-body system, Science **353**, 794 (2016).

[16] A. J. Daley, H. Pichler, J. Schachenmayer, and P. Zoller, Measuring Entanglement Growth in Quench Dynamics of Bosons in an Optical Lattice, Phys. Rev. Lett. **109**, 020505 (2012).

[17] T. Brydges, A. Elben, P. Jurcevic, B. Vermersch, C. Maier, B. P. Lanyon, P. Zoller, R. Blatt, and C. F. Roos, Probing Rényi entanglement entropy via randomized measurements, Science **364**, 260 (2019).

[18] H. Pichler, L. Bonnes, A. J. Daley, A. M. Läuchli, and P. Zoller, Thermal versus entanglement entropy: a measurement protocol for fermionic atoms with a quantum gas microscope, New J. Phys. **15**, 063003 (2013).

[19] E. Cornfeld, E. Sela, and M. Goldstein, Measuring fermionic entanglement: Entropy, negativity, and spin structure, Phys. Rev. A **99**, 062309 (2019).

[20] B. Swingle, Entanglement Entropy and the Fermi Surface, Phys. Rev. Lett. **105**, 050502 (2010).

[21] More precisely, we define $|A|$ to include spin/orbital degeneracies so that $V|A|$ is the number of modes in A. We note that the heuristic argument for a volume law is confirmed by the more detailed all-orders diagrammatic calculation provided in the Supplemental Material [22].

[22] See Supplemental Material at http://link.aps.org/supplemental/10.1103/PhysRevB.107.L081109 for the supplemental material provides a diagrammatic proof of equation (9), which holds to all orders in the interaction strength U.

[23] B. Fang, A. Johnson, T. Roscilde, and I. Bouchoule, Momentum-Space Correlations of a One-Dimensional Bose Gas, Phys. Rev. Lett. **116**, 050402 (2016).

[24] S. S. Hodgman, R. I. Khakimov, R. J. Lewis-Swan, A. G. Truscott, and K. V. Kheruntsyan, Solving the Quantum Many-Body Problem via Correlations Measured with a Momentum Microscope, Phys. Rev. Lett. **118**, 240402 (2017).

[25] H. Cayla, C. Carcy, Q. Bouton, R. Chang, G. Carleo, M. Mancini, and D. Clément, Single-atom-resolved probing of lattice gases in momentum space, Phys. Rev. A **97**, 061609(R) (2018).

[26] C. Carcy, H. Cayla, A. Tenart, A. Aspect, M. Mancini, and D. Clément, Momentum-Space Atom Correlations in a Mott Insulator, Phys. Rev. X **9**, 041028 (2019).

[27] P. M. Preiss, J. H. Becher, R. Klemt, V. Klinkhamer, A. Bergschneider, N. Defenu, and S. Jochim, High-Contrast Interference of Ultracold Fermions, Phys. Rev. Lett. **122**, 143602 (2019).

[28] A. Sterdyniak, A. Chandran, N. Regnault, B. A. Bernevig, and P. Bonderson, Real-space entanglement spectrum of quantum Hall states, Phys. Rev. B **85**, 125308 (2012).

[29] F. Schindler, N. Regnault, and B. A. Bernevig, Exact quantum scars in the chiral nonlinear Luttinger liquid, Phys. Rev. B **105**, 035146 (2022).

[30] I. Mondragon-Shem, M. Khan, and T. L. Hughes, Characterizing Disordered Fermion Systems using the Momentum-Space Entanglement Spectrum, Phys. Rev. Lett. **110**, 046806 (2013).

[31] E. C. Andrade, M. Steudtner, and M. Vojta, Anderson localization and momentum-space entanglement, J. Stat. Mech.: Theory Exp. (2014) P07022.

[32] B.-T. Ye, Z.-Y. Han, L.-Z. Mu, and H. Fan, Investigating disordered many-body system with entanglement in momentum space, Sci. Rep. **7**, 16668 (2017).

[33] R. Lundgren, F. Liu, P. Laurell, and G. A. Fiete, Momentum-space entanglement after a quench in one-dimensional disordered fermionic systems, Phys. Rev. B **100**, 241108(R) (2019).

[34] R. Thomale, D. P. Arovas, and B. A. Bernevig, Nonlocal Order in Gapless Systems: Entanglement Spectrum in Spin Chains, Phys. Rev. Lett. **105**, 116805 (2010).

[35] R. Lundgren, J. Blair, M. Greiter, A. Läuchli, G. A. Fiete, and R. Thomale, Momentum-Space Entanglement Spectrum of Bosons and Fermions with Interactions, Phys. Rev. Lett. **113**, 256404 (2014).

[36] M. Ibáñez-Berganza, J. Rodríguez-Laguna, and G. Sierra, Fourier-space entanglement of spin chains, J. Stat. Mech.: Theory Exp. (2016) 053112.

[37] B. Dóra, R. Lundgren, M. Selover, and F. Pollmann, Momentum-Space Entanglement and Loschmidt Echo in Luttinger Liquids after a Quantum Quench, Phys. Rev. Lett. **117**, 010603 (2016).

[38] Y.-M. Wei and H. Lu, General interaction quenches in a Luttinger liquid, Commun. Theor. Phys. **74**, 015702 (2022).

[39] A. Anfossi, P. Giorda, and A. Montorsi, Momentum-space analysis of multipartite entanglement at quantum phase transitions, Phys. Rev. B **78**, 144519 (2008).

[40] G. Ehlers, J. Sólyom, O. Legeza, and R. M. Noack, Entanglement structure of the Hubbard model in momentum space, Phys. Rev. B **92**, 235116 (2015).

[41] V. Balasubramanian, M. B. McDermott, and M. Van Raamsdonk, Momentum-space entanglement and renormalization in quantum field theory, Phys. Rev. D **86**, 045014 (2012).

[42] T.-C. L. Hsu, M. B. McDermott, and M. Van Raamsdonk, Momentum-space entanglement for interacting fermions at finite density, J. High Energy Phys. 11 (2013) 121.

[43] B. Han and R. Akhoury, Entanglement, renormalization and effective field theories, arXiv:2011.05380.

[44] S. Kawamoto and T. Kuroki, Momentum-space entanglement in scalar field theory on fuzzy spheres, J. High Energy Phys. 12 (2021) 101.

[45] I. Peschel, Letter to the Editor: Calculation of reduced density matrices from correlation functions, J. Phys. A: Math. Gen. **36**, L205 (2003).

[46] S. Moitra and R. Sensarma, Entanglement entropy of fermions from Wigner functions: Excited states and open quantum systems, Phys. Rev. B **102**, 184306 (2020).

[47] A. Haldar, S. Bera, and S. Banerjee, Rényi entanglement entropy of Fermi and non-Fermi liquids: Sachdev-Ye-Kitaev model and dynamical mean field theories, Phys. Rev. Res. **2**, 033505 (2020).

[48] See Ref. [18] for additional comments regarding ordering ambiguities and Ref. [19] for the generalization to higher Rényi entropies.

[49] I. Bloch, J. Dalibard, and W. Zwerger, Many-body physics with ultracold gases, Rev. Mod. Phys. **80**, 885 (2008).

[50] T. Giamarchi, *Quantum Physics in One Dimension*, International Series of Monographs on Physics (Clarendon Press, Oxford, UK, 2004).

[51] K. A. Hallberg, New trends in density matrix renormalization, Adv. Phys. **55**, 477 (2006).

[52] U. Schollwöck, The density-matrix renormalization group in the age of matrix product states, Ann. Phys. **326**, 96 (2011).

[53] J. I. Cirac, D. Pérez-García, N. Schuch, and F. Verstraete, Matrix product states and projected entangled pair states: Concepts, symmetries, theorems, Rev. Mod. Phys. **93**, 045003 (2021).
[54] T. Xiang, Density-matrix renormalization-group method in momentum space, Phys. Rev. B **53**, R10445 (1996).
[55] J. Motruk, M. P. Zaletel, R. S. K. Mong, and F. Pollmann, Density matrix renormalization group on a cylinder in mixed real and momentum space, Phys. Rev. B **93**, 155139 (2016).
[56] G. Ehlers, S. R. White, and R. M. Noack, Hybrid-space density matrix renormalization group study of the doped two-dimensional Hubbard model, Phys. Rev. B **95**, 125125 (2017).
[57] M. B. Hastings, I. González, A. B. Kallin, and R. G. Melko, Measuring Renyi Entanglement Entropy in Quantum Monte Carlo Simulations, Phys. Rev. Lett. **104**, 157201 (2010).
[58] Z. H. Liu, G. Pan, X. Y. Xu, K. Sun, and Z. Y. Meng, Itinerant quantum critical point with fermion pock-ets and hotspots, Proc. Natl. Acad. Sci. USA **116**, 16760 (2019).
[59] X. Zhang, G. Pan, Y. Zhang, J. Kang, and Z. Y. Meng, Momentum space quantum monte carlo on twisted bilayer graphene, Chin. Phys. Lett. **38**, 077305 (2021).